Structural Investigation of Mercury-Intercalated Titanium Disulfide. 1. The Crystal Structure of $Hg_{1.24}TiS_2$

P. Ganal,† P. Moreau,† G. Ouvrard,*,† M. Sidorov,‡ M. McKelvy,‡ and W. Glaunsinger§,‡

Institut des Matériaux de Nantes (I.M.N.), 2, rue de la Houssinière, 44072 Nantes, France; Center for Solid State Science, Arizona State University, Tempe, Arizona 85287-1704; and Department of Chemistry and Biochemistry, Arizona State University, Tempe, Arizona 85287-1604

Received October 27, 1994. Revised Manuscript Received March 21, 1995®

X-ray powder and single-crystal diffraction have been used together with thermogravimetric compositional analysis to determine the crystal structure of the superstoichiometric intercalation compound $Hg_{1.24}TiS_2$ at ambient temperature. $Hg_{1.24}TiS_2$ forms an unusual (3 + 1)-dimensional layered misfit compound, which can alternatively be described as interpenetrating three-dimensional TiS_2 and Hg sublattices. The symmetry of each sublattice can be described by the monoclinic space group *C*2/*m*. These sublattices share commensurate *a* and *c* axes but are incommensurate with each other along the *b* axis [$a = 5.9223(9)$ Å, $b_{TiS_2} = 3.4076(2)$ Å, $b_{Hg} = 2.7566(1)$ Å, $c = 8.862(1)$ Å, and $\beta = 102.33(3)°$]. Hg forms infinite one-dimensional chains within the nearly trigonal prismatic sulfur channels created by host-layer restacking. The Hg chains exhibit metallic intrachain guest–guest bonding, with a bond distance of 2.76 Å. Comparison of the intrachain Hg–Hg bond distance to the Hg^{n+}–Hg^{n+} bond distances for compounds containing linear Hg chains with a known ionic valence indicates the intercalated Hg in $Hg_{1.24}TiS_2$ has very little ionic character. Unlike other transition-metal dichalcogenide intercalation compounds that possess primarily ionic guest–host interactions, this compound exhibits weak covalent guest–host interactions and very little ionic charge transfer.

Introduction

1T-TiS_2 is a model two-dimensional material whose chemical and physical properties are largely governed by its bonding anisotropy. Like many other layered transition metal dichalcogenides (TMDs), it consists of chalcogenide–TM–chalcogenide lamella[1–3] and crystallizes in the CdI_2 structure (space group $P\bar{3}m1$, $a = 3.4073$ Å, $c = 5.6953$ Å).[4] Each TiS_2 lamella is composed of a hexagonal titanium layer whose atoms are located at the octahedral sites defined by its neighboring hexagonal close-packed sulfur layers. Within the TiS_2 lamella strong covalent titanium–sulfur bonds are formed, whereas interlayer bonding consists of weak van der Waals (vdW) interactions. Due to the electron-accepting potential of TiS_2 and the weak interlayer interaction between the lamella, a broad spectrum of atomic and molecular guests can be intercalated between the host layers.[2,3,5]

One of the most intensely investigated classes of guests that form TMD intercalation compounds (TMDICs) are the elemental metals.[2,3] These intercalants are generally believed to form ionic guests and occupy discrete lattice sites in the vdW gap. However, recent studies have revealed that mercury-intercalated TMDICs possess some novel properties that cannot be explained within this general description.[6–12] These properties include the ability to intercalate "superstoichiometric"[13] levels of Hg in monolayer form (e.g., Hg_xTiS_2, where $x > 1.00$) with an interlayer expansion of ~3 Å, weak electronic guest–host interactions that appear to be primarily covalent in character, and the indication of unusually complex structures based on X-ray powder diffraction, which suggest a fundamental difference from other metal (M)–TMDICs.[6–9,11] Previ-

† Institut des Matériaux de Nantes.
‡ Center for Solid State Science, ASU.
§ Department of Chemistry and Biochemistry, ASU.
® Abstract published in *Advance ACS Abstracts,* April 15, 1995.

(1) Balchin, A. A. In *Crystallography and Crystal Chemistry of Materials with Layered Structures*; Lévy, F., Ed.; D. Reidel: Dordrecht, Holland, 1976; p 1.
(2) Lévy, F., Ed. *Intercalated Layered Materials*; D. Reidel: Dordrecht, Holland, 1979.
(3) Whittingham, M. S., Jacobson, A. J., Eds. *Intercalation Chemistry*; Academic Press: New York, 1982.
(4) Chianelli, R. R.; Scanlon, J. C.; Thompson, A. H. *Mater. Res. Bull.* **1975**, *10*, 1379.
(5) Friend, R. H.; Yoffe, A. D. *Adv. Phys.* **1987**, *36*, 1.
(6) Ong, E. W. Ph.D. Thesis, Arizona State University, Tempe, AZ, 1990.
(7) McKelvy, M.; Sharma, R.; Ong, E.; Burr, G.; Glaunsinger, W. *Chem. Mater.* **1991**, *3*, 783.
(8) Ong, E. W.; McKelvy, M. J.; Ouvrard, G.; Glaunsinger, W. S. *Chem. Mater.* **1992**, *4*, 14.
(9) Moreau, P.; Ouvrard, G. *Chemical Physics of Intercalation II*; Bernier, P., Fischer, J. E., Roth, S., Solin, S. A., Eds.; Plenum Press: New York, 1993; Nato ASI Series Vol. 305, p 351.
(10) Ganal, P.; Olberding, W.; Butz, T.; Ouvrard, G. *Chemical Physics of Intercalation II*; Bernier, P., Fischer, J. E., Roth, S., Solin, S. A., Eds.; Plenum Press: New York, 1993; Nato ASI Series Vol. 305, p 383.
(11) Moreau, P.; Ganal, P.; Ouvrard, G. *Mol. Cryst. Liq. Cryst.* **1994**, *244*, 325.
(12) McKelvy, M.; Sidorov, M.; Marie, A.; Sharma, R.; Glaunsinger, W. *Chem. Mater.* **1994**, *6*, 2233, and in press.
(13) The guest species generally reside in octahedral or trigonal prismatic sites in metal–TMDICs, resulting in a maximum guest uptake of $x = 1.00$ for these monolayer intercalates. The term "superstoichiometric" refers to the formation of single-guest-layer compounds with $x > 1.00$.

0897-4756/95/2807-1132$09.00/0

ous investigations also indicate the presence of an incommensurate Hg sublattice, for which several interlayer structural models have been suggested.[6,11,14] Although the Hg−TMDICs Hg_xNbSe_2 and Hg_xTaS_2 were first prepared in the early 1970s,[15,16] no complete structure analysis has been published for any of these compounds.

An unusual structural feature of some mercury-containing compounds is the presence of nearly linear incommensurate mercury chains formed by relatively strong mercury metal−metal bonding. Such chains were first reported for the nonstoichiometric compound $Hg_{2.82}AsF_6$ by Brown et al. in 1974.[17] Although some related compounds have been discovered since then,[18−21] the formation of solid-state structures containing incommensurate metallic mercury chains (i.e., with metallic intrachain bonding) seemed to be limited to the $Hg_{3-\delta}MF_6$ (M = As, Sb, Ta, Nb) family of compounds.[21] Recently, we have discovered that the nonstoichiometric mercury intercalates of titanium disulfide also contain similar, nearly linear, chainlike mercury arrangements,[22] which suggests that the formation of infinite Hg chains in solids is a more general phenomenon than previously realized. Herein and in the following paper,[22] we present the mercury intercalates of titanium disulfide as the first example of a new class of compounds in which similar chainlike Hg arrangements are found.

To investigate the complex structural properties of these new materials, we have combined the complementary techniques of X-ray diffraction (XRD) and high-resolution transmission electron microscopy (HRTEM). In this paper (1) we report the structure of $Hg_{1.24}TiS_2$ as determined by X-ray powder diffraction (XPD) and confirmed by single-crystal XRD. In the following paper (2), we describe our HRTEM investigation of the evolution of the intercalate structure during Hg deintercalation.

Experimental Section

TiS_2 single crystals and powders were prepared directly from the elements at 913 K using excess sulfur.[23] XPD was routinely employed to confirm the synthesis of highly stoichiometric host materials, since the *c* lattice parameter of titanium disulfide is a function of composition ($Ti_{1+x}S_2$).[24] The host material was prepared and handled under inert conditions, since prior air exposure of the host inhibits Hg intercalation. Mercury intercalation was usually carried out at ambient temperature by mixing the disulfide with a slight excess of liquid mercury under inert conditions. Ambient-temperature Hg intercalation occurred spontaneously and rapidly for both powders and single crystals and was typically complete in several minutes, as judged by the vanishing of the added Hg and a slight darkening of the golden color of the host. To ensure complete intercalation as well as the long-term stability of the intercalation product, samples were stored in contact with excess Hg. Exact molar ratios of Hg and TiS_2 (1.24:1.00) were also reacted to form XPD samples of $Hg_{1.24}TiS_2$. For these studies, highly stoichiometric TiS_2 ($Ti_{1.002}S_2$) was sealed together with the appropriate amount of Hg in a sealed quartz ampule at 10^{-4} Torr. The ampule was then heated at 593 K for a few days followed by slow cooling to ambient temperature. The resulting intercalate was a free-flowing powder.[6−8]

Thermogravimetric analysis (TGA) was performed using either a Perkin-Elmer TGS-2 thermogravimetric analysis system or a Setaram TG92 thermal analysis system. A Perkin-Elmer DSC4 was used for differential scanning calorimetry experiments. Intercalate compositions were determined by TGA in an inert Ar or He atmosphere, as described previously.[6−8]

XPD measurements were performed using the Debye−Scherrer geometry on an INEL powder diffractometer[25,26] equipped with a position-sensitive, curved CPS120 detector and a bent quartz monochromator. The incident X-ray beam was monochromatic Cu K-L_3 radiation (λ = 1.540 598 Å) generated by a sealed copper X-ray tube operated at 40 kV and 30 mA. The diffractometer was calibrated with cubic $Na_2Ca_3Al_2F_{14}$ to give an overall accuracy of about $\delta_{2\theta}$ = 0.009°.[26] To minimize the effects of preferred orientation and the high absorption coefficient of Hg, crystalline powders of less than 50 μm grain size were attached to the exterior of small Lindeman capillaries (o.d. = 0.1 mm) with vacuum grease. Some measurements were also performed in the Bragg−Brentano geometry on a Siemens D5000 diffractometer. Essentially the same results were obtained for the Rietveld refinement of data taken with either diffractometer. However, preferred orientation was a problem with the latter diffractometer. As a result, the data taken with the INEL diffractometer was chosen for the final data analysis presented herein. The XPD patterns obtained with the INEL diffractometer were calibrated to a constant 2θ step width of 0.03° using the PROLIX and/or PXRAY programs,[25,27] together with the known reflections of cubic $Na_2Ca_3Al_2F_{14}$. The structure analysis was based on a Rietveld-type refinement of the entire pattern and was performed using both the MPROF-program chain[28] and the FULLPROF program.[29]

Single-crystal X-ray diffraction studies were performed using a Weissenberg camera (*R* = 2.8648 cm, Cu K-L_{23} radiation).

Results

Characterization. The compositions of the intercalates prepared with excess Hg(l) at ambient temperature were difficult to determine by TGA alone, since the transition from the vaporization of Hg(l) to the deintercalation of Hg_xTiS_2 is hard to resolve. The inability to resolve these events is associated with the similar enthalpies (14 kcal/mol of Hg) for the heat of vaporization of Hg(l) and the deintercalation of Hg from Hg_xTiS_2.[8] However, samples with a nominal composi-

(14) Tröger, W.; Butz, T.; Ouvrard, G. *Hyperfine Interact.* **1993**, *80*, 1149.
(15) Tracey, T.; Gentile, P. S.; Budnick, J. T. *ONR Conference on the Physics and Chemistry of Layered Compounds*; Conference Abstracts, Monterey, CA, Aug 17, 1972.
(16) Di Salvo, F. J.; Hull Jr., G. W.; Schwartz, L. H.; Voorhoeve, J. M.; Waszczak, J. V. *J. Chem. Phys.* **1973**, *59*, 1922.
(17) Brown, I. D.; Cutforth, B. D.; Davies, C. G.; Gillespie, R. J.; Ireland, P. R.; Vekris, J. E. *Can. J. Chem.* **1974**, *52*, 791.
(18) Schultz, A. J.; Williams, J. M.; Miro, N. D.; MacDiarmid, A. G.; Heeger, A. J. *Inorg. Chem.* **1978**, *17*, 646.
(19) Tun, Z.; Brown, I. D. *Acta Crystallogr.* **1982**, *B38*, 2321.
(20) Brown, I. D.; Gillespie, R. J.; Morgan, K. R.; Tun, Z.; Ummat, P. K. *Inorg. Chem.* **1984**, *23*, 4506.
(21) Brown, I. D.; Datars, W. R.; Gillespie, R. J.; Morgan, K. R.; Tun, Z.; Ummat, P. K. *J. Solid State Chem.* **1985**, *57*, 34.
(22) Sidorov, M.; McKelvy, M.; Sharma, R.; Glaunsinger, W.; Ganal, P.; Moreau, P.; Ouvrard, G. *Chem. Mater.*, following article in this issue.
(23) McKelvy, M. J.; Glaunsinger, W. S. *J. Solid State Chem.* **1987**, *66*, 181.
(24) Thompson, A. H.; Gamble, F. R.; Symon, C. R. *Mater. Res. Bull.* **1975**, *10*, 915.
(25) Deniard, P.; Evain, M.; Barbet, J. M.; Brec, R. *Mater. Sci. Forum* **1991**, *79−82*, 363.
(26) Evain, M.; Deniard, P.; Jouanneaux, A.; Brec, R. *J. Appl. Crystallogr.* **1993**, *26*, 563.
(27) Ganal, P. PXRAY: a program for XPD data format conversion, I.M.N., Nantes, France, 1993.
(28) Murray, A. D.; Fitch, A. N. MPROF: a Multipattern Rietveld Refinement Program for Neutron, X-ray and Synchrotron Radiation; SERC Daresbury Laboratory, Warrington, England, 1992.
(29) Rodriguez-Carvajal, J. *Fullprof*, a program for profile refinement of constant-wavelength X-ray and neutron powder diffraction patterns, Institut Laue Langevin, Grenoble, France, 1992.

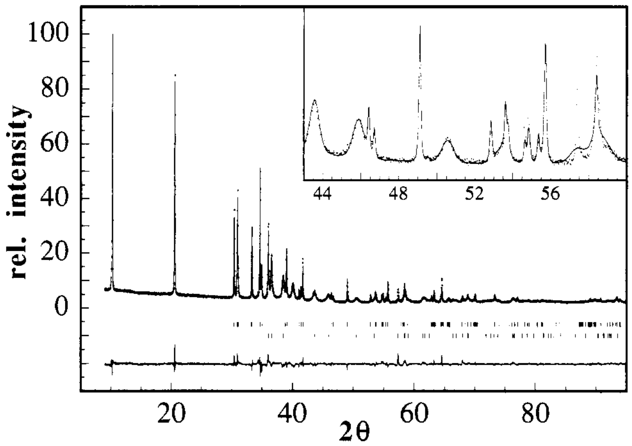

Figure 1. Observed (points) and calculated (solid line) X-ray powder diffraction patterns for $Hg_{1.24}TiS_2$ at ambient temperature. The calculated pattern is generated by Rietveld refinement using the two-phase composite crystal approach discussed in the text. The difference profile is shown at the bottom. An enhanced view of the region from 43 to 60° is shown in the upper right corner. The reflections were separated into two groups: (1) those solely associated with the TiS_2 sublattice and those common to both sublattices and (2) those only due to the Hg sublattice. The upper marks between the observed pattern and the difference profile correspond to the TiS_2 sublattice and common peak positions. The lower marks correspond to the Hg sublattice peaks.

tion of $x < 1.23$ did not exhibit a thermal event at the Hg solid−liquid phase transition (244 K) during DSC analysis, whereas those with $x > 1.23$ did, indicating a maximum value of x near 1.23. This is within experimental error of the maximum possible Hg uptake corresponding to $x = 1.24$ based on the observed structure, as discussed later, indicating the presence of an equilibrium between $Hg_{1.24}TiS_2$ and Hg(l) for samples prepared at ambient temperature. This value for the maximum uptake of Hg is somewhat lower than the value of $Hg_{1.29}TiS_2$ reported previously for samples prepared at 593 K and slowly cooled to ambient temperature.[6,8] However, the latter composition was determined by TGA alone, which is less precise than using the TGA/DSC procedure described above.

The sample composition of materials prepared using a 1.24:1.00 molar ratio of Hg:TiS_2 was determined by inert-atmosphere TGA.[6−8] The resulting sample compositions are summarized by the formula $Hg_{1.24\pm0.01}TiS_2$. The intercalation process was thermally reversible both compositionally and structurally, as judged by oxidative thermal analysis and XPD of the deintercalated TiS_2, respectively.[6,8]

X-ray Powder Diffraction. XPD patterns for $Hg_{1.24}TiS_2$, as shown in Figure 1, contain sets of sharp and broad reflections that can be generally associated with the TiS_2 and Hg sublattices, respectively. These sublattices have no simple commensurate relation and have been previously indexed to separate monoclinic lattices rotated by 5° with respect to each other.[11] However, a parallel nonequilibrium investigation of partially deintercalated Hg_xTiS_2 by HRTEM revealed monoclinic TiS_2 and Hg sublattices that share common a and c axes and are only incommensurate along the b axis.[22] Following similar reasoning for the equilibrium compound $Hg_{1.24}TiS_2$, a complete integer indexing of the entire XPD pattern is possible in (3 + 1)-dimensional superspace.[30] The positions of the Bragg reflections can thus be

Table 1. X-ray Powder Diffraction Data for $Hg_{1.24}TiS_2$

h	$k1$	l	$k2$	$d_{obs}{}^a$ (Å)	d_{hkl} (Å)	I_{obs}	I_{calc}
0	0	1	0	8.663	8.6400	100	100
0	0	2	0	4.328	4.3247	72	69
−2	0	1	0	2.939	2.9370	18	16
2	0	0	0		2.8906	10	9
0	0	3	0	2.887	2.8843	29	26
−1	1	1	0		2.8752	3	3
−2	0	2	0	2.684	2.6829	15	16
2	0	1	0	2.583	2.5817	31	30
−1	1	2	0	2.565	2.5609	6	7
1	0	0	1	2.488	2.4874	17	15
−1	0	1	1	2.452	2.4507	15	15
1	0	1	1	2.335	2.3341	12	12
−2	0	3	0	2.304	2.3025	12	12
−1	0	2	1	2.247	2.2474	10	11
2	0	2	0	2.198	2.1970	2	2
−1	1	3	0	2.179	2.1787	4	3
0	0	4	0	2.165	2.1632	11	11
1	0	2	1	2.076	2.0756	7	8
−1	0	3	1	1.976	1.9755	6	6
1	1	3	0	1.954	1.9542	2	2
−2	0	4	0	1.943	1.9427	2	1
2	0	3	0	1.855	1.8540	6	7
1	0	3	1	1.804	1.8038	4	4
0	0	5	0	1.732	1.7309	2	2
−1	0	4	1	1.713	1.7123	3	3
−3	1	1	0	1.707	1.7076	2	2
0	2	0	0	1.703	1.7031	1	1
3	1	0	0	1.679	1.6778	1	1
−3	1	2	0	1.672	1.6727	1	1
0	2	1	0		1.6710	1	1
1	1	4	0	1.657	1.6579	1	2
−2	0	5	0	1.649	1.6484	6	6
−3	0	1	1	1.605	1.6043	3	2
3	0	0	1	1.578	1.5797	2	2
2	0	4	0		1.5784	4	3
−3	0	2	1	1.574	1.5752	2	2

^{a} The observed d spacings, d_{obs}, have been determined by single reflection refinements using the Prolix program.[25] The d_{hkl} spacings as well as the intensities I_{obs} and I_{calc} were obtained from the final Rietveld refinement using the MPROF program.[28]

described by the vector expression $H = ha^* + k_1b^*_{TiS_2} + 1c^* + k_2b^*_{Hg}$, with $b^*_{Hg} = \alpha(b^*_{TiS_2})$ and $\alpha \approx 1.236$. The incommensurability of the b lattice parameters accounts quantitatively for the 5° rotation found between the Hg and TiS_2 ($hk0$)−sublattice reflections [$\arctan(a/b_{Hg}) - \arctan(a/b_{TiS_2}) = 5°$].[11]

The indexing of the d spacings for $Hg_{1.24}TiS_2$ is shown in Table 1, while the lattice parameters and relevant crystallographic data are summarized in Table 2. The systematic absence of reflections with $h + k_1 \neq 2n$ and $h + k_2 \neq 2n$ indicates that the TiS_2 and Hg sublattices are C-face centered, respectively, which suggests the three-dimensional space group $C2$ or $C2/m$ for each sublattice.[32,33]

A composite crystal approach was used for the initial refinement of the average structure. This approach involves the separation of the XPD reflections into three subsets: (1) the $(h,k_1,l,0)$ reflections with $k_1 > 1$ that are generated only by the TiS_2 sublattice, (2) the

(30) Janssen, T.; Janner, A.; Looijenga-Vos, A.; Wolff, P. U. In *International Tables for Crystallography*; Wilson, A. J. C., Ed.; Kluwer Academic Publishers: Dordrecht, Holland, 1992; p 797.

(31) Thompson, P.; Cox, D. E.; Hastings, J. B. *J. Appl. Cryst.* **1987**, *20*, 79.

(32) By definition, there is no three-dimensional space group that describes the total symmetry of an incommensurate composite crystal. An appropriate symmetry description of the $Hg_{1.24}TiS_2$ crystal structure requires a (3 + 1)-dimensional space group.[33] However, the symmetry of each sublattice can be described by the three-dimensional space groups used herein.

(33) Ganal, P.; Ouvrard, G., to be published.

Table 2. Crystallographic Data for $Hg_{1.24}TiS_2$

chemical formula[a]	$Hg_{1.24}TiS_2$
formula mass (amu)	360.0
space group[b]	*C*2/*m* (No. 12)
cell parameters	
a (Å)	5.9223(9)
b_{TiS_2} (Å)	3.4076(2)
b_{Hg} (Å)	2.7566(1)
c (Å)	8.862(1)
β (deg)	102.33(3)
V_{TiS_2} (Å^3)	174.7(1)
V_{Hg} (Å^3)	141.3(1)
Z	2
ϱ_{calc} (g/cm^3)[a]	6.84
XPD diffractometer	INEL, CPS120 detector
radiation	Cu K-L$_3$, quartz monochromator
λ (Å)	1.540 598
abs coeff. μ_a (cm^{-1})	131.3
calibration	external $Na_2Ca_3Al_2F_{14}$ standard
$2\theta_{max}$	115°
temp (K)	293
refinement method	Rietveld least-squares analysis
weighting scheme	$1/(y_{obs} + y_{back})$
no. of parameters	43
line-shape profiles	
TiS_2 part	split Pearson VII
Hg part	parametrized pseudo-Voigt[c]
R_I[d]	6.13
R_{wp}[d]	7.43
χ^2[d]	5.34

[a] Calculated from the lattice parameters. [b] For each sublattice. [c] Thompson et al.[31] [d] Defined as $R_I = 100\Sigma_i|I_i - I_{ci}|/\Sigma_i|I_i|$, $R_{wp} = 100\sqrt{\Sigma_i w_i(y_i - y_{ci})^2/\Sigma_i w_i y_i^2}$, and $\chi^2 = (R_{wp}/R_{ex})^2$.

$(h,0,l,k_2)$ reflections with $k_2 > 1$ that arise solely from the Hg sublattice, and (3) the $(h,0,l,0)$ reflections common to both sublattices. Because the Hg and TiS_2 sublattices are incommensurate, there is on average no constructive interference between the three reflection subsets, so they can be analyzed in terms of three different phases. The three parts were refined concurrently, while constraining the individual a, c, and β lattice parameters to be common to each subset. The line shapes of the TiS_2 and common reflections were described by a Split–Pearson VII profile,[34] and the Hg reflections were described by a parameterized pseudo-Voigt profile.[31] To reduce the number of free parameters, the scale factor and profile parameters for the TiS_2 reflections were constrained to be equal to those for the common reflections in this refinement. A slight modification of the classical composite crystal approach, creating a two-phase model, was then applied avoiding the latter constraints in the final refinement. In this model, the TiS_2 sublattice reflections and the reflections common to both sublattices are treated as a single phase. This was accomplished by incorporating a highly anisotropic temperature factor of $U_{2.2} = 20$ for the Hg atoms in the TiS_2 sublattice in order to simulate a uniform Hg-atom distribution along the b-axis direction.

Compared with the classical-composite-crystal approach, the two-phase model resulted in slightly better values for R_I, R_{wp}, and χ^2 and reasonable values for the atomic thermal parameters. The atomic scattering factors and dispersion corrections for Ti, S, and Hg were taken from the "International Tables for X-Ray Crystallography".[35] The observed XPD intensities were corrected for Lorentz and monochromator polarization effects prior to refinement, and the diffuse background of the XPD pattern was fitted with a Fourier polynomial of the 12th order. The atomic positions calculated for a hypothetical 3*R* mercury titanium disulfide intercalation compound with AbC CaB BcA host-layer stacking were used as a starting point for the refinements. Either *C*2 or *C*2/*m* was used for the space group for both the two-phase and three-phase reflection subsets. Since the symmetry of the Hg and TiS_2 sublattices are equally well described by the space groups *C*2 and *C*2/*m*, the distinction between *C*2 and *C*2/*m* is relevant only for common reflections and for constraining the origin of the Hg sublattice. If the origin is located on the special crystallographic position $(^1/_4,y,^1/_2)$ relative to the TiS_2 sublattice shown in Table 3, then the space group is *C*2/*m*. The choice of the y coordinate is arbitrary, since the reflections common to both sublattices consist only of $(h,0,l,0)$ reflections, consistent with the Hg and TiS_2 sublattices being incommensurate along their parallel b axes. The final results of the two-phase Rietveld refinement are summarized in Tables 1–4.[36] An illustration of the observed and calculated XPD patterns and their difference profile is given in Figure 1. Schematic illustrations of the crystal structure, depicting the nearly trigonal-prismatic stacking of the host layers about the parallel Hg chains are shown in Figure 2.

Table 3. Atomic Coordinates and Thermal Parameters of $Hg_{1.24}TiS_2$

(a) (TiS_2) and (Common) Part

Positional Parameters

atom	position	x	y	z	B_{iso} (Å^2)	occupancy
Ti	2(a)	0	0	0	1.9(3)	1
S	4(i)	0.387(1)	0	0.166(1)	1.0(2)	1
Hg	4(f)	0.25	a	0.5		0.617(4)

Anisotropic Thermal Parameters

atom	$U_{1.1}$	$U_{2.2}$	$U_{3.3}$	$U_{1.2}$	$U_{1.3}$	$U_{2.3}$
Hg	0.038(1)	20[a]	0.0020(3)	0	−0.0018(4)	0

(b) (Hg) Part

Positional Parameters

atom	position	x	y	z	B_{iso} (Å^2)	occupancy
Hg	2(a)	0	0	0	4.1(2)	1

[a] The y coordinate of Hg was chosen as 0.25 together with a fixed value of $U_{2.2} = 20$ to simulate the random y coordinates of the Hg positions in the TiS_2 sublattice due to the incommensurate b axes of the TiS_2 and Hg sublattices.

The excellent agreement between the peak intensities, as shown for the representative lower-angle reflections in Table 1, for all of the reflections demonstrates the reliability of the general structure. However, as illustrated by Table 1 and the inset in Figure 1, although the overall peak intensities (and positions) are well described by the refinement, many of the peak shapes are not, providing the primary contribution to the relatively high values for R_{wp}, and χ^2. The $Hg_{1.24}TiS_2$ diffraction peaks are often much broader and more

(34) Toraya, H. *J. Appl. Crystallogr.* **1986**, *19*, 440.
(35) MacGillavry, C. H., Rieck, G. D., Eds. *International Tables for X-ray Crystallography*: Kynoch Press: Birmingham, England, 1968; Vol. III.

(36) Other host-layer stacking schemes, such as AbC BaC AcB, with nearly octahedral coordination of the guest layers are also consistent with the monoclinic host sublattice parameters and can explain all of the diffraction peak positions. However, they cannot account for the peak intensities. Structure refinements for such arrangements were unable to reduce χ^2 below 35.

Table 4. Atomic Distances and Angles for $Hg_{1.24}TiS_2$[a]

distance (Å)		angle (deg)	
Ti(1)–Ti(1)	3.4076(2)	Ti(1)–Ti(1)–Ti(1)	180
Ti(1)–Ti(2)	3.4163(2)	Ti(1)–Ti(2)–Ti(1)	59.83
Ti(1)–S(1)	2.443(5)		
Ti(1)–S(3)	2.436(5)		
S(1)–S(1)	3.4076(2)	S(1)–Ti(2)–S(1)	88.8(2)
S(1)–S(2)	3.416(7)	S(1)–Ti(2)–S(2)	88.9(2)
S(1)–S(3)	3.483(7)	S(1)–Ti(2)–S(3)	91.1(2)
S(1)–S(4)	3.481(9)	S(1)–Ti(2)–S(4)	91.2(2)
Hg(1)–Hg(1)	2.7566(1)	Hg(1)–Hg(1)–Hg(1)	180
Hg(1)–Hg(2)	3.2663(2)	Hg(1)–Hg(2)–Hg(1)	49.9

[a] The Hg–S distance depends on the actual position of the Hg atom with respect to the TiS_2 sublattice and varies continuously between $d_{min} = 3.23$ Å at $y_{Hg} = 0$ and $d_{max} = 3.36$ Å at $y_{Hg} = 0.269$ (see Figure 5).

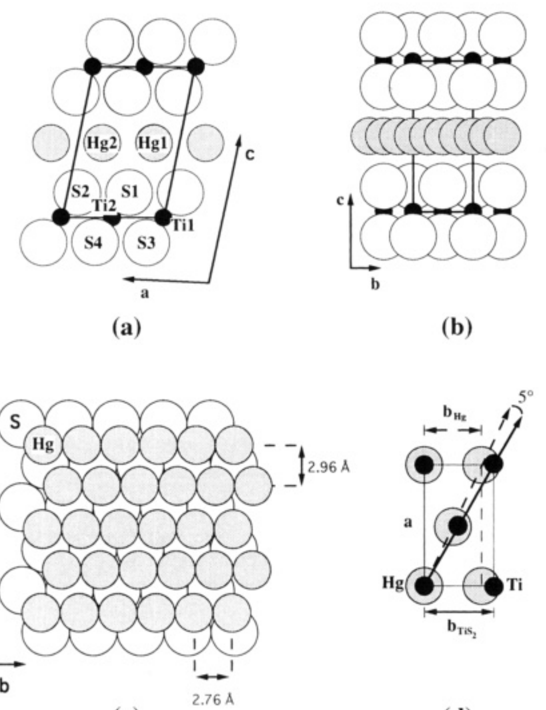

Figure 2. Schematic illustrations of the $Hg_{1.24}TiS_2$ crystal structure: (a) projection along the *b* axis showing the interlayer structure viewed parallel to the Hg chains; (b) a projection along the *a* axis showing the interlayer structure viewed perpendicular to the chains; (c) a projection perpendicular to the layers showing the relative intralayer arrangement of the Hg atoms with respect to a neighboring S layer; (d) superposition of the TiS_2 and Hg inplane unit cells showing the 5° rotation between the $(\boldsymbol{a} + \boldsymbol{b})_{Hg}$ and $(\boldsymbol{a} + \boldsymbol{b})_{TiS_2}$ sublattice diagonals.

asymmetric than those observed for pristine TiS_2. For example, the reflections from the Hg sublattice usually exhibit a Hendricks–Teller-like behavior,[37] with most of these reflections broadening considerably with increasing diffraction angle, while others, such as the (0,0,0,2) reflection, remain sharp. Such peak profiles typically indicate the presence of high concentrations of intrinsic structural imperfections, such as the stacking faults and Hg-sublattice domains observed for Hg_xTiS_2 by HRTEM in paper 2.[22] Since these intrinsic structural imperfections cannot be incorporated into the refinement, their effects on the resulting peak shapes will increase the values of R_{wp} and χ^2.

(37) Hendricks, S.; Teller, E. *J. Chem. Phys.* **1942**, *10*, 147.

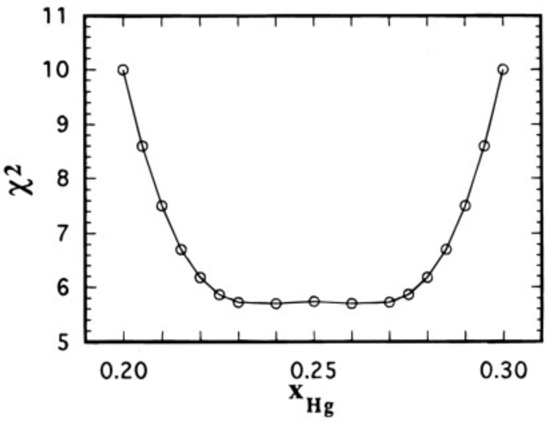

Figure 3. x cross section through the χ^2 surface of the Rietveld refinement showing the similar fit for $0.23 \le x \le 0.27$ in the three-phase refinement ($R_I = 7.46$, $R_{wp} = 7.84$, $\chi^2 = 5.78$) suggesting the x coordinate of the Hg chains is not well defined. The x coordinate of the Hg chains could not be refined with the two-phase model, because of its strong correlation with $U_{1.1}$.

*C*2 was chosen instead of *C*2/*m* as the space group for the common part of the three-phase refinement in order to refine the x and z coordinates of the Hg positions. As expected from symmetry considerations, the z coordinate remained at $z = 0.5$. However, the x coordinate was found to vary between 0.22 and 0.28, depending on the refinement procedure. The χ^2 surface confirms the x coordinate of the Hg positions is not well defined, as shown in Figure 3, with χ^2 being essentially independent of x for $0.23 \ge x \ge 0.27$. In the two-phase model used for the final refinement this observation corresponds to the fairly large anisotropy of the Hg temperature factors ($U_{1.1} \gg U_{3.3}$, Table 3). Both the poorly defined x coordinates of the average Hg positions in the three-phase refinement and the large value of $U_{1.1}$ resulting from the two-phase model can be related, as discussed later, to a-axis modulations of the Hg positions (transverse to the b, Hg chain, axis) similar to those observed for Hg_xTiS_2.[22] Both the χ^2 surface shown in Figure 3 and the anisotropy of the Hg temperature factors are consistent with such modulations having an amplitude of the order of 0.2 Å. The two-phase refinement allowed a slightly better description of these modulations. However, such modulations cannot be generally described by the composite crystal approach and, hence, contribute to the relatively high refinement controls.

Another factor which may contribute to the magnitude of R_I, R_{wp}, and χ^2 is the value used for the absorption correction. This value, $\mu_a R = 1.65$, is a best estimate, since it was not possible to accurately measure the thickness of the crystalline layer coating adhered to the exterior of the glass capillary.

Single-Crystal X-ray Diffraction. Due to the deterioration of crystal quality that accompanies Hg intercalation, the Weissenberg films exhibited streaking of diffraction spots characteristic of the presence of stacking faults. However, on rotating-crystal films the reflections were spotlike and were used as a stringent test of the XPD indexing. The films were analyzed using the SIMWEIS program,[38] which simulates Bragg

(38) Ganal, P. "Computer Simulations of Weissenberg Photographs", unpublished results.

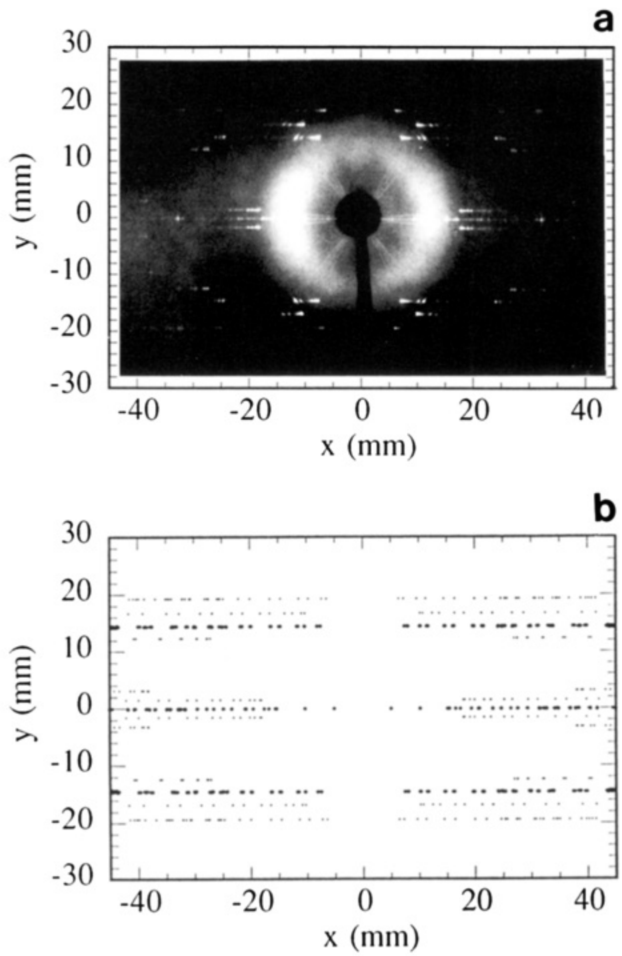

Figure 4. Rotating-crystal photograph of a $Hg_{1.24}TiS_2$ single crystal taken with a Weissenberg camera is shown on top (a). The crystal was rotated along a hexagonal axis, a_h, of the TiS_2 host lattice. Within the pseudo-hexagonal description, this corresponds to the diagonal $(\boldsymbol{a} + \boldsymbol{b})_{TiS_2}$. A computer simulation of a rotating-crystal photograph using the XPD crystal structure information given in Table 3 and the same rotational axis as in (a) is shown on the bottom (b). The reflections from the TiS_2 host lattice and those common to both sublattices are represented by the larger spots. All of the reflections on the experimental film can be accounted for by the presence of three symmetry-related Hg domains rotated by 120° with respect to each other, as discussed in the text.

and Weissenberg film patterns for a given set of lattice parameters. Using the crystal shape as a guide, the single crystals were usually oriented such that the rotation axis of the Weissenberg camera was parallel to a hexagonal axis of the original TiS_2 host lattice (i.e., the a_h axis). This corresponds to either the monoclinic b axis or the TiS_2 sublattice diagonal given by $(\boldsymbol{a} + \boldsymbol{b})_{TiS_2}$ for $Hg_{1.24}TiS_2$. The corresponding diagonal of the Hg sublattice, $(\boldsymbol{a} + \boldsymbol{b})_{Hg}$, is rotated by about 5° from $(\boldsymbol{a} + \boldsymbol{b})_{TiS_2}$, as shown in Figure 2d. Therefore, each TiS_2 layer line should be closely associated with two layer lines arising from the Hg sublattice, which is exactly what is observed experimentally, as shown in Figure 4. Further confirmation of the structure derived from the refinement of XPD data comes from the alignment of the rotation axis along the Hg sublattice diagonal and the a and b axes of the monoclinic lattice. All of these rotating-crystal film studies were in excellent agreement with the crystal structure determined by XPD.

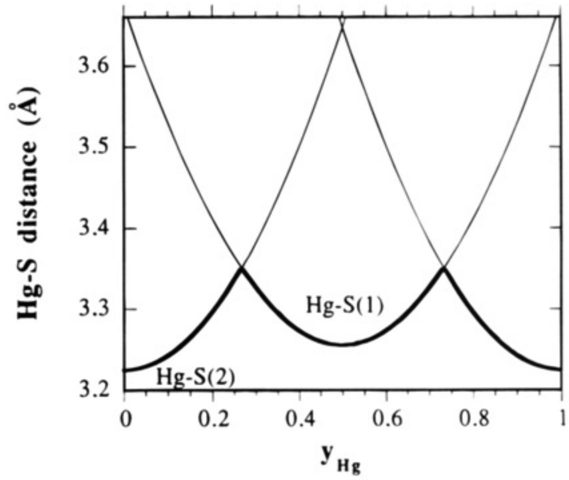

Figure 5. Nearest-neighbor Hg–S distances are indicated by the dark line as a function of the y coordinate of the Hg position, y_{Hg}, within the TiS_2 sublattice unit cell. The continuous variation between 3.23 and 3.36 Å depends on the local incommensurate Hg position in the TiS_2 sublattice.

Discussion

Structure of $Hg_{1.24}TiS_2$. TiS_2 intercalation is often accompanied by a restacking of the host layers from octahedral to trigonal-prismatic coordination of the guest sites in the vdW gap associated with the formation of a 3*R* structure with AbC CaB BcA stacking.[5] A similar host-layer restacking is found for $Hg_{1.24}TiS_2$, in which the nearest-neighbor TiS_2 host layers are shifted along the a-axis direction of the monoclinic TiS_2 sublattice by approximately $2a/3$ to provide nearly trigonal prismatic coordination of the guest sites. This results in a planar network of linear sulfur channels rotated by 120° with respect to each other in the vdW gap. The intercalated Hg atoms form infinite one-dimensional chains that occupy these relatively open sulfur channels. The relatively short Hg-Hg distance along the direction of the chains, b = 2.757 Å, is associated with Hg–Hg bonding and is much smaller than the interchain Hg–Hg distance of 3.266 Å. Since the Hg and TiS_2 sublattices are incommensurate along b, the y coordinates of the Hg positions vary from one host-layer cell to another and, therefore, cannot be defined relative to the TiS_2 sublattice. This results in nearest-neighbor Hg–S distances varying continuously between 3.23 and 3.36 Å, depending on the local Hg position in the TiS_2 sublattice, as shown in Figure 5. Complete space filling of these channels by the Hg chains gives a maximum theoretical Hg uptake for the ambient-temperature $Hg_{1.24}TiS_2$ structure of 1.24 mol of Hg/mol of TiS_2.

The Hg chains can also be viewed in terms of their three-dimensional ordered sublattice structure. The parallel chains in $Hg_{1.24}TiS_2$ are separated by 2.961 Å, as shown in Figure 2c. Both their intrachain Hg–Hg distances and their interchain separation offer interesting comparisons with those observed for the perpendicular, nonintersecting Hg-metal chains in $Hg_{3-\delta}MF_6$ (M = As, Sb, Ta, Nb), where these distances are significantly smaller (2.67 ± 0.01 Å) and larger (3.23 ± 0.01 Å), respectively.[18,21,39] The longer intrachain Hg–Hg distance in $Hg_{1.24}TiS_2$ can be related to its reduced

(39) Pouget, J. P.; Shirane, G.; Hastings, J. M.; Heeger, A. J.; Miro, N. D.; MacDiramid, A. G. *Phys. Rev. B* **1978**, *18*, 3645.

Hg valence, as discussed below, whereas the much shorter distance between the chains can be related to stronger interchain ordering interactions. Unlike $Hg_{3-\delta}AsF_6$, where the Hg chains only order at low temperatures (≤120 K),[39] the Hg chains in $Hg_{1.24}TiS_2$ are ordered at ambient temperature. These stronger interchain interactions in $Hg_{1.24}TiS_2$ are not surprising, as its planar arrangement of parallel Hg chains with a smaller interchain distance should allow stronger interchain interactions than the more widely spaced, orthogonal stacking of nonintersecting Hg chains in $Hg_{3-\delta}AsF_6$.[21,39]

The presence of significant guest–host interlayer interactions follows directly from the observation of three-dimensional, ordered guest and host sublattices. These three-dimensional interactions are probably not associated with interlayer electrostatic repulsions, since these intercalates exhibit at most only very weak ionic character, as discussed in the following section. Instead, it seems more probable that the three-dimensional ordering of the Hg and TiS_2 sublattices is related to local structural modulations associated with Hg–S interactions.[22]

As suggested by the reversibility of the intercalation process,[6–8] the TiS_2 layers are little affected by Hg intercalation, with the Ti atoms retaining their octahedral sulfur coordination. However, the Ti–S bond lengths for $Hg_{1.24}TiS_2$, shown in Table 4, are slightly longer than those for TiS_2 (2.4279(1) Å),[4] which is likely a direct effect of Hg–S bonding.

Hg–S bonding may also be associated with the poorly defined x coordinate of the Hg chains indicated in Figure 3. This behavior may be correlated to a modulation of the Hg positions transverse to their chain-axis direction to optimize the combined Hg–S guest–host and Hg–Hg guest–guest interactions. Such an in-plane modulation has been observed directly by HRTEM for Hg_x·TiS_2 intercalates.[22] Similar undulations have been observed for the infinite Hg chains relative to the MF_6 framework in $Hg_{3-\delta}MF_6$ (M = As, Sb, Ta, Nb).[21]

In contrast to the general behavior of M–TMDICs, the crystal structure of $Hg_{1.24}TiS_2$ also exhibits a pronounced monoclinic distortion, which further underscores the unusual guest–host interactions in this compound. This distortion from the ideal 3R structure has two components. First, the host-layer restacking glide shift of the TiS_2 lamella differs by about 0.1 Å from that expected for an ideal 3*R* stacking sequence. Second, there is a slight 0.02 Å elongation of the a axis, which breaks the hexagonal symmetry of the TiS_2 layers. These distortions indicate there is some, presumably covalent, interaction between the incommensurate Hg chains and their sulfur environment depicted in Figure 2a–c. The imperfect glide shift is probably a result of attractive interactions between the Hg chains and their S channels. In contrast, the a elongation may be associated with a repulsive interaction between nearest-neighbor Hg chains.

As mentioned earlier, the Hg chains can be oriented along any of three symmetry-related directions in the nearly trigonal prismatically coordinated sulfur channels. This suggests the possibility of three equivalent Hg domains rotated by 120° with respect to each other, which have been observed directly by HRTEM.[22] Such domains had to be included in the modeling of the single-crystal X-ray data in order to completely reproduce the experimental patterns.

The structure of $Hg_{1.24}TiS_2$ also provides new insight into a recent time-differential perturbed angular correlation study of Hg_xTiS_2.[14] The observed asymmetry of the electric-field gradient, $\eta = 0.41$, in this study apparently arises from the different directions of the two sublattice contributions, with the contribution from the incommensurate Hg chains being directed along the b axis and the contribution from the TiS_2 layers mainly oriented along the c axis. It is also apparent that Hg does not occupy a single site, as suggested previously.[14] This is likely associated with the inability to resolve the continuous shift of the Hg sites relative to the host lattice in the former study, which may be partly due to the off-chain-axis modulation of the Hg positions associated with local Hg–S interactions.

Guest–Host Electronic Interactions. There is substantial Hg–Hg bonding in $Hg_{1.24}TiS_2$ based on the intrachain Hg–Hg distance. This bonding appears to be analogous to that found in the low-temperature crystal structure of β-Hg.[40] In particular, the (110) planes of β-Hg bear a strong resemblance to the intralayer arrangement of Hg chains in $Hg_{1.24}TiS_2$, with the former material having similar intrachain and interchain Hg–Hg distances of 2.825 and 3.158 Å, respectively. This suggests that $Hg_{1.24}TiS_2$ possesses similar metallic Hg–Hg bonding to that found in the neutral-Hg structure.

Previous ion exchange, redox intercalation, and host-layer S diameter studies suggest the presence of at most a very low level of ionic charge transfer and the possibility of weak covalent electron exchange for Hg_xTiS_2.[6,8] A subsequent magnetic susceptibility investigation of Hg_xTiS_2 indicates the presence of significant guest–host interactions but could not conclusively determine the nature of the interactions.[9,11] A parallel X-ray absorption near-edge structure comparison of $Hg_{1.24}TiS_2$ with $Li_x^+TiS_2^{x-}$ revealed that the guest–host interaction is not a simple ionic interaction but instead is better described as primarily covalent in nature.[9,11] This follows from the position of the Ti K edge for TiS_2 being essentially unaffected by the intercalation of Hg, which is in contrast to the behavior observed for the ionic intercalates $Li_x^+TiS_2^{x-}$, where the Ti K edge continuously shifts to lower energies with increasing x.[9,11]

A direct comparison of the intrachain Hg–Hg distance in $Hg_{1.24}TiS_2$ to that in compounds containing structurally isolated, metal–metal-bonded, linear Hg chains with known ionic Hg character should provide valuable insight into the electronic guest–host interactions that drive the Hg–TiS_2 intercalation process. Such a comparison of intrachain Hg–Hg distances as a function of Hg charge transfer is shown in Figure 6. The observed intrachain Hg–Hg distances for each class of compounds is essentially unaffected by their specific anionic environments. Therefore, they are well suited for the

(40) Atoji, M.; Schirber, J. E.; Swendson, C. A. *J. Chem. Phys.* **1959**, *31*, 1628.
(41) Torsi, G.; Fung, K. W.; Begun, G. H.; Manatov, G. *Inorg. Chem.* **1975**, *10*, 2285.
(42) Cutforth, B. D.; Davies, C. G.; Dean, P. A. W.; Gillespie, R. J.; Ireland, P. R.; Ummat, P. K. *Inorg. Chem.* **1973**, *12*, 1343.
(43) Cutforth, B. D.; Gillespie, R. J.; Ireland, P. R.; Sawyer, J. F.; Ummat, P. K. *Inorg. Chem.* **1983**, *22*, 1344.

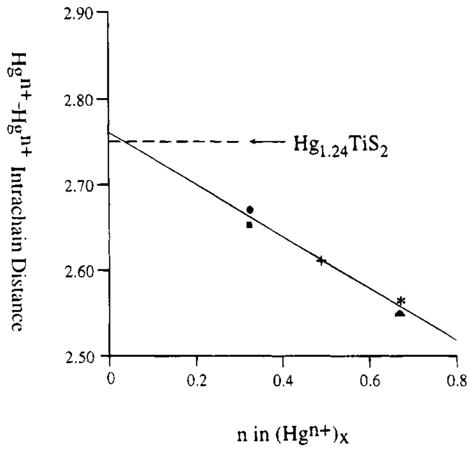

Figure 6. Comparison of intrachain $Hg^{n+}-Hg^{n+}$ bond distances as a function of n for compounds containing linear Hg chains. The $Hg_{1.24}TiS_2$ intrachain distance is shown as a horizontal dashed line. The data shown are for the three-atom Hg_3^{2+} ($n = 2/3$) chains in $Hg_3(AlCl_4)_2$ (*)[41] and $Hg_3(AsF_6)_2$ (▲),[42] the four-atom Hg_4^{2+} ($n = 1/2$) chains in $Hg_4(AsF_6)_2$ (+),[43] and the infinite linear $(Hg^{1/3+})_\infty$ chains in $Hg_{3-\delta}(MF_6)$ [M = As, Nb, Ta (●) and Sb (■)].[21] The intrachain Hg–Hg distance used for $Hg_4(AsF_6)_2$ (2.61 Å) is the average of the three bond distances in its four-atom Hg_4^{2+} chains (2.62, 2.59, and 2.62 Å).[43]

analysis of Hg–Hg bond distances as a function of linear cation valence to investigate the ionic character of the incommensurate chains in $Hg_{1.24}TiS_2$. The Hg–Hg intrachain distance observed for $Hg_{1.24}TiS_2$ is shown as a straight dashed line. A linear relationship exists between the seven ionic compounds having a known Hg valence of Hg^{n+}. Extrapolation of this relationship suggests very weak ionic character for $Hg_{1.24}TiS_2$, with $n \sim 0.04$, consistent with the presence of primarily covalent guest–host interactions.

β-Hg has not been included in Figure 6 because interchain interactions, which can increase the intrachain Hg–Hg distance, are important in this compound. The intrachain distance for neutral Hg in the low-temperature β-Hg structure at 77 K is 2.82 Å,[40] which is somewhat larger than that observed for $Hg_{1.24}TiS_2$. Inclusion of this point in the analysis shown in Figure 6 would result in an increased, but still weak, ionic component for intercalated Hg in TiS_2. However, the presence of unscreened bonding between the chain atoms in β-Hg and the eight nearest-neighbor interchain atoms at a distance of 3.158 Å is likely to contribute significantly to the higher intrachain Hg–Hg distance in β-Hg.[40] This expectation is supported by the rhombohedral structure of α-Hg,[40,44] where each atom has six nearest neighbors at 2.993 Å at 78 K. In this case, the Hg atoms can also be considered as "chains", where their shorter interchain Hg–Hg distances relative to β-Hg can be associated with longer intrachain Hg–Hg distances and weaker intrachain bonding.

(44) Barrett, C. S. *Acta Crystallogr.* **1957**, *10*, 58.

Conclusion

The results of this study demonstrate that Hg–TMDICs are very unusual intercalation compounds. $Hg_{1.24}TiS_2$ has a novel (3 + 1)-dimensional misfit structure, unlike any other known M–TMDIC structure. This structure can be described as two interpenetrating Hg and TiS_2 sublattices that share commensurate monoclinic a and c axes but are incommensurate along their common b axis. Metallic guest–guest bonding in this compound results in the formation of one-dimensional Hg chains. This metallic bonding is relatively strong, as the intrachain Hg–Hg bond distance of 2.757 Å is somewhat shorter than the intrachain bond distance in β-Hg (2.825 Å).[40] Comparison with the intrachain bond distances found for solid-state Hg compounds with known ionic character indicates that intercalated Hg possesses very little ionic character, so that Hg-bonding interactions primarily involve weak covalent guest–host and metallic guest–guest interactions.

The structural investigation of Hg–TMDICs is complex. As discussed in this paper, although the peak positions and intensities for $Hg_{1.24}TiS_2$ are in excellent agreement with the refined structure, the peak shapes give rise to rather high values for R_I, R_{wp}, and χ^2, associated with the local modulations of the Hg positions and the presence of intrinsic structural imperfections that cannot be accommodated in the refinement. The identification and structure of these modulations and structural imperfections such as three equivalent Hg domains rotated by 120° and stacking faults, which have been suggested herein, are discussed in the following paper on the HRTEM investigation of Hg_xTiS_2.[22]

Acknowledgment. It is a pleasure to thank Prof. J. Rouxel for his continuous interest and support. This work was supported by a Conseil Régional des Pays de la Loire grant (P.G.). We wish to acknowledge the National Science Foundation for support through Grants DMR 91-06792 and INT-8914990, and acknowledgment is made to the donors of The Petroleum Research Fund, administered by the American Chemical Society, for partial support of this research. P.G. is especially grateful to V. Maisonneuve for his help in beginning the Rietveld refinements.

Supplementary Material Available: Tables with a complete indexation of the X-ray powder diffraction data and structure factors (hk_1lk_2, F^2_{obs}, F^2_{calc}, $\sigma|F|$) (5 pages). Ordering information is given on any current masthead page.

CM9404881